香港天文台
HONG KONG OBSERVATORY

Reprint 871

Latest Developments of Windshear Alerting Services at the Hong Kong International Airport

P.W. Chan, C.M. Shun & M.L. Kuo

14th Conference on Aviation, Range, and Aerospace Meteorology,
American Meteorological Society, Atlanta, Georgia,
USA, 17-21 Jan 2010

10.4 Latest developments of windshear alerting services at the Hong Kong International Airport

P.W. Chan *, C.M. Shun and M.L. Kuo
Hong Kong Observatory, Hong Kong, China

1. INTRODUCTION

Low-level windshear and turbulence could be hazardous to the aircraft. At the Hong Kong International Airport (HKIA), windshear and turbulence alerts are issued if they are expected to occur below a height of 1600 feet or within 3 nautical miles away from the respective runway end. Windshear alerting services at HKIA are provided by the Hong Kong Observatory (HKO). A number of algorithms have been developed to give automatic windshear alerts, such as the anemometer-based alerts and the LIDAR Windshear Alerting System (LIWAS). With all such efforts, the hit rate of pilot windshear reports has got to about 90% in the recent years with the alert duration per hit on a decreasing trend.

Despite the generally satisfactory performance of the windshear alerting services, enhancement works are still on-going in a number of aspects. On the windshear alerting side, LIWAS algorithm has only been developed for arrival runway corridors and the corresponding algorithm for departure runway corridors needs to be established. In particular, the length of the windshear ramp appears to be a critical factor in setting up the alerting criterion. The existing windshear algorithms are mainly based on wind data collected by the LIDARs and the surface-based anemometers. The use of other remote-sensing instruments, such as the spectral width data of the Terminal Doppler Weather Radar (TDWR) in rain and the thermodynamic profiles provided by a ground-based microwave radiometer, would need to be explored. Moreover, there is increasing concern on the effect of buildings on the low-level airflow and the building-associated turbulence should be measured as well.

Another major issue with the development of windshear/turbulence alerting services is the establishment of the “sky truth” dataset based on which the alerting algorithms are established. At the moment, the pilot reports of low-level windshear and turbulence form the most important source of the “sky truth”. However, they are prone to subjective judgement of the pilots and more objective dataset would be useful in determining the quantitative relationship between the magnitude of windshear/turbulence and the meteorological data measured at the time of the event. To this end, HKO obtains the Quick Access Recorder (QAR) data from the local airlines and conducts collaborative study with the National Aerospace Laboratory (NLR) in the Netherlands to develop the software for calculating windshear and turbulence quantities out of the flight data. The meteorological measuring system of a fixed-wing aircraft of the Government Flying Service (GFS) of the Hong Kong Government has also been upgraded recently to collect wind data at a high frequency (up to 20 Hz) in order to provide the sky truth data of windshear and turbulence within the planetary boundary layer.

This paper summarizes the above-mentioned developments in the last year or so at HKIA for improving windshear and turbulence alerting services. Some preliminary results of these studies would be given.

2. DUAL LIWAS

The LIWAS algorithm has been used operationally for the arrival runway corridors of HKIA since 2005. The technical details of the algorithm could be found in Shun and Chan (2008). With a single LIDAR working at the air traffic control complex of HKIA, the algorithm did not perform so well for the most used departure runway corridor of HKIA in the spring-time windshear season (namely, departing from the south runway of HKIA to the east, 07RD) because the laser beam has a rather large angle (more than 30 degrees) with respect to the runway orientation around the rotation point of the aircraft.

Dual LIWAS has been established at HKIA since early 2008, namely, one LIDAR serving a specific runway of the airport. A schematic diagram of dual LIWAS is shown in Figure 1. Under this configuration, the laser beam of each LIDAR is better aligned with the respective runway. Data are also updated more frequently, namely, headwind profile for a particular runway corridor is available every 1 – 2 minutes. With the improvement of data coverage, LIWAS algorithm is optimized for 07RD by making reference to the pilot windshear reports. An intensive observation period of 07RD windshear occurrence was conducted in liaison with the Hong Kong air traffic control (ATC) and local airlines in the spring of 2009.

The length of windshear ramp detected by the LIDAR could be a critical factor in considering the issuance of windshear alerts (see the discussions in Shun and Chan (2008)). In the development of LIWAS algorithm for 07RD, two cut-off lengths of windshear ramps have been examined, namely, the conventional value of 4 km in the existing LIWAS algorithm (4 km is based on the maximum length used in the alerting of microburst by the TDWR) and a shorter length of 3 km. The impact of different ramp lengths on hit rate, false alarm rate and alert duration are considered. The study results of LIWAS for the spring and early summer of 2009 (January to May) are summarized in Tables 1 and 2. For the departure runway corridors (07RD, and 25LD viz. departing from the south runway of HKIA to the west), the use of a short ramp length (3 km) does not change the hit rate very much, but could result in much shorter alert duration and smaller false alarm rate. The latter is

* *Corresponding author address:* P.W. Chan, Hong Kong Observatory, 134A Nathan Road, Hong Kong email: pwchan@hko.gov.hk

particularly evident for 25LD runway corridor over which ATC has helped to collect a significant number of null windshear reports for algorithm development purpose. The performance of LIWAS for the arrival runway corridors in the study period is given in Table 2. In general, LIWAS performs well with a hit rate of about 80% and a false alarm rate of 34% or less. The hit rate for 25RA (arriving at the north runway of HKIA from the east) is rather low in the study period because of the extended failure of the north runway LIDAR (note: the hit rate of 07LA is not very much affected because the windshear mostly occurred beyond 1 nm, which was well covered by the south runway LIDAR).

It is noted that, though with improved alignment between the laser beam of the LIDAR and the runway orientation, the hit rate of 07RD windshear is about 2/3 only. The missed cases have been studied whenever QAR data are available. Some examples of missed cases are shown in Figure 2. There are a number of reasons for the misses, namely, (a) the headwind change measured by the LIDAR is slightly less than that encountered by the aircraft (see Figure 2(a)), probably because of the transient and sporadic nature of terrain-induced airflow disturbances, (b) the measurement range of the LIDAR is limited due to the low cloud base (see Figure 2(b)), and (c) both aircraft and LIDAR do not show significant windshear whereas the pilot perceives the occurrence of significant windshear with subjectivity (see Figure 2(c)). For the three reasons, point (b) is more related to the instrumentation limitation that may not be improved with the use of the LIDAR technology alone. The use of more sophisticated technologies, such as cloud radar that measures the winds within clouds, may need to be explored in order to fully capture the headwind profile along the flight path in humid and cloudy conditions.

3. MICROWAVE RADIOMETER

The windshear algorithms developed for HKIA are mainly based on wind measurements – both the point measurements by surface-based anemometers and remote-sensing data such as LIDAR and TDWR. The terrain-induced airflow disturbances could be associated with changes in the thermodynamic profile of the lower troposphere as well, and the development of windshear algorithms has been explored with the continuous availability of temperatures within the boundary layer. Such temperature data have been collected by a number of thermometers installed at HKIA, along the slopes as well as on the mountain top of Lantau Island. Moreover, temperature profiles up to 10 km above ground are obtained in real time from a ground-based microwave radiometer (Figure 3a).

The radiometer uses 7 oxygen channels to retrieve the tropospheric temperature profile (Chan, 2009). In particular, elevation scans are performed to obtain high-resolution temperature data within the planetary boundary layer. The latter is particularly useful in detecting changes of the temperature profile during the occurrence of cross-mountain airflow. An example of the profile in a windshear event is shown in Figure 3b. In the morning of 20 January 2009, there were 47 reports of significant windshear over 07LA (arriving at the north runway of HKIA from the west) and 07RD. A temperature inversion of about 1 degree Celsius could be seen between 250 and 650 m above ground. The cross-mountain airflow at that time may have resulted in the warming of an elevated layer of the air within the boundary layer. The 3.2-degree conical scan of the LIDAR in the early morning of 20 January 2009 is shown in Figure 3c. An east to southeasterly jet is discernible over the airport and a mountain wake (lighter winds coloured in brown to grey) could be analyzed to the west of HKIA. This windshear event is a typical case of terrain-disrupted airflow in spring-time. The combined use of LIDAR and microwave radiometer data could give the aviation weather forecasters more confidence in the issuance of manual windshear warnings.

4. SHORT-RANGE LIDAR

Apart from the mountains, buildings may also result in disturbances in the low-level winds to be encountered by the landing/departing aircraft. A study of the potential effects of buildings on the low-level winds was conducted in the summer of 2009 by setting up a short-range LIDAR on the rooftop of an exhibition centre (Figure 4a). This LIDAR has 20 range gates with a selectable gate size between 30 and 75 m. As such, it can measure the radial velocity of the wind up to a maximum range of 600 to 1500 m. It is more suitable than the existing LIDARs in the measurement of building-associated turbulence because of the small gate size (the existing LIDARs have a gate size of 105 m) and more frequent data update (every 20 seconds versus 1 – 2 minutes of the existing LIDARs). The scanning area of this short-range LIDAR with respect to the 25RA flight path is shown in Figure 4b. This LIDAR makes horizontal scan only within a sector size of about 40 degrees in azimuth, and the scan plane is just below the arriving aircraft over 25RA.

The LIDAR data could be used in a number of ways, for instance, the radial velocity plot over the 40-degree sector scan to show the variation of wind speed, the 2D wind field derived from the radial velocity using VAD (Velocity Azimuth Display) technique to show the airflow disturbances, and the 2D turbulence intensity map. For the last application, the eddy dissipation rate (EDR) is calculated based on the radial velocity data. EDR is the internationally adopted turbulence intensity metric for aviation applications. Two examples of EDR maps are shown in Figure 5. Each map is computed using a sub-sector size of 10 range gates, around 7 beams of data over a period of 5 minutes. Technical details of the computation method could be found in Chan and Kwong (2008).

In the first case, light south to southeasterly winds affected the northeastern part of HKIA island over which the exhibition centre is located (Figure 5a). The EDR map is given in Figure 5b. $EDR^{1/3}$ is larger within the first couple of hundred metres or so from the LIDAR, reaching a maximum value of about 0.19 $m^{2/3}s^{-1}$. It decreases at further distances away from the building, dropping to below 0.1 $m^{2/3}s^{-1}$ at about 500 m. This pattern of $EDR^{1/3}$ could be expected because of the more turbulent airflow closer to the building and lighter turbulence at larger distance away

in the south to southwesterly flow situation.

The second case is the moderate to fresh southeasterly flow associated with a departing tropical cyclone (Figure 5c). The EDR values are in general larger (Figure 5d) than those of the first case. Severe turbulence (EDR of about 0.5 $m^{2/3}s^{-1}$) occurs at close range of the LIDAR and EDR drops to the level of moderate turbulence at 450 to 600 m away from the LIDAR (about 0.3 $m^{2/3}s^{-1}$).

The EDR maps in the two cases appear to be reasonable. QAR data are being obtained to provide more quantitative verification of the EDR values.

5. TDWR-BASED EDR MAP

In the existing Windshear and Turbulence Warning System (WTWS) of HKIA, turbulence intensity along the flight path is computed based on the ground-based anemometer readings. Attempts have been made to calculate EDRs over the flight paths using LIDAR data (e.g. Chan and Kwong (2008)). The LIDAR-derived EDR would be useful in the alerting of turbulence in clear-air conditions. The next step would be the computation of EDR for rainy weather, and the spectral width data of TDWR is a natural choice for this application.

Technical details of the TDWR-based EDR could be found in Zhang et al. (2009). The lowest elevation scans of the TDWR, namely, 0.6-degree conical scans, are considered. The scanning area with respect to the flight paths is shown in Figure 6. EDR has been computed with and without the inclusion of the windshear term. The resulting EDR values (both median and maximum) within a distance of 5 nautical miles away from the runway end have been compared with the corresponding values obtained from the QAR data (see Section 6 below) for a total of 14 flights. The comparison has been conducted for both 07LA and 25RA runway corridors (the most used arrival corridors of HKIA). The comparison results are given in Figure 7.

In general, the median EDR values of the two datasets (TDWR and QAR) compare reasonably well. As such, the TDWR-based EDR is considered to capture the “general” turbulence level along the flight paths. On the other hand, the maximum EDR values of the two datasets do not compare so well. There could be a couple of reasons for that: firstly the maximum EDR value may appear as a single peak only in the turbulence profile along the flight path and such a peak could be highly transient and sporadic in the turbulent airflow; secondly, the 0.6-degree conical scans of TDWR do not cover exactly the locations of the flight paths, and there could be significant differences in altitudes between the aircraft and the radar beam (e.g. when an aircraft over 25RA touches the ground of about 7 m above the sea level, the TDWR beam is situated at about 140 m).

The present sample size (14 flights) is still too small to conclude whether the removal of the windshear term would be useful in the calculation of TDWR-based EDR. A larger dataset covering various kinds of weather conditions (scattered thunderstorms, and rains associated with tropical cyclones, etc.) would be considered in future studies.

An example of the TDWR EDR map is shown in Figure 8a. The corresponding maps of spectral width, radar reflectivity and radial velocity are given in Figures 8b to d respectively. Severe turbulence appears over the airport. This is in general consistent with the EDR profile analyzed from the QAR data, as depicted in Figure 9. Generally speaking, the TDWR and QAR EDRs do not compare so well at larger distances away from the runway end, e.g. there is a peak of severe turbulence between 3.5 and 4 nautical miles away from the runway end in the QAR data, whereas the turbulence remains light to moderate in the TDWR data. The height difference between the radar beam and the flight path could be a possible reason for this discrepancy.

6. QAR DATA ANALYSIS

In collaboration with NLR, a software package, called WINDSTURB, has been developed to process the QAR data available from airlines and obtain the required meteorological quantities taking into account the aerodynamic factors of the aircraft types commonly operated by the airlines (namely, A320, A330, B747 and B777). The meteorological parameters for low-level windshear and turbulence applications include, among others, the three components of the wind, windshear hazard factor (F-factor), and EDR. Technical details of the algorithm could be found in Haverdings and Chan (2009).

A main feature of the data analysis software is the application of Kalman filtering and smoothing. It is a process of estimating the state vector of a dynamical system at a particular stage and its covariance by using the measurements at all stages. The Kalman filter-smoother in the present algorithm is used specifically to estimate the inertial vertical speed as accurately as possible, which is an element of the state vector that is estimated, consisting of 3 velocities, 3 positions and 3 accelerometer biases. Measurements used are inertial data (e.g. track, groundspeed), attitudes (Euler angles), drift angle, pressure and radio altitudes, etc.

The F-factor is calculated by considering the rate of headwind change as well as the vertical acceleration. 5-second average value is calculated. The F-factor derived from QAR data has been compared with that estimated from the headwind profiles measured by the LIDAR systems at HKIA, from which only the rate of headwind change term of F-factor could be calculated. The comparison result for the absolute maximum value over the last 4 nautical miles of aircraft landing at HKIA is given in Figure 10a. It could be seen that both datasets show reasonable correlation. Thus, with the support of the F-factor determined from QAR data, the LIDAR systems have the potential of providing the windshear hazard factor, in addition to the headwind change itself, for real-time alerting purpose. This is being studied using pilot windshear reports over a period of several years.

The wind-based EDR calculation method is implemented in the software. As derived from the

first principle of turbulence, the calculation of EDR requires the solution of the power spectrum in the inertial sub-range of the vertical wind component over a selected time window with a certain vertical mean velocity. A more practical method, as implemented in the software, is to employ a running-mean standard deviation calculation of the bandwidth-filtered vertical wind with two cut-off frequencies. The resulting EDR is compared with that determined from the LIDAR radial velocity data, with the median $EDR^{1/3}$ values considered over the last 4 nautical miles of aircraft landing at HKIA. Though they are measuring different components of the wind (vertical wind for QAR vs. essentially horizontal wind in the LIDAR measurements), the two sets of EDR data are found to have reasonably good correlation (Figure 10b). The results demonstrate the potential for using LIDAR in the detection of low-level turbulence.

7. RESEARCH FLIGHTS

Fixed-wing aircraft (Jetstream 4100) is used by GFS in search and rescue operations. Its onboard flight management system provides meteorological data, including the horizontal winds and the temperature, but they are found to be not accurate enough for the purpose of windshear and turbulence studies. In mid-2009, the meteorological measuring system of a Jetstream 4100 aircraft has been upgraded. The new system, based on Aircraft-Integrated Meteorological Measurement System (AIMMS-20), outputs the three components of the wind in 20 Hz with an accuracy of 0.5 m/s for the horizontal wind components and 1 m/s for the vertical wind component in straight and level flights. Apart from the winds, AIMMS-20 also provides temperature, humidity and pressure data.

The setup of the system on the fixed-wing aircraft is shown in Figure 11a. Two GPS antennae are installed at the tips of the wings. Under the left wing, an air data probe (inset of Figure 11a) is set up to make the raw meteorological measurements. The measurement data are transmitted into the components inside the cabin, including a GPS module, an inertial measurement unit and a data processing unit, for calculating the meteorological parameters and storing the output data.

A comparison of headwind data measured by the LIDAR and the fixed-wing aircraft is shown in Figure 11b (over 07LA runway corridor). It could be seen that the two datasets are very well correlated.

8. CONCLUSIONS

This paper discusses a number of new developments in windshear and turbulence alerting services in Hong Kong in the last year or so. There are two major aspects in such development works. First of all, the alerting methodology has been improved by using a variety of remote-sensing instruments, such as LIDAR, TDWR and microwave radiometer. Secondly, the collection of “sky truth” windshear and turbulence data has been enhanced. More objective data are obtained, which would be useful in the establishment of quantitative algorithms in the alerting of both windshear and turbulence.

The topics presented in this paper are on-going development activities of HKO. More detailed discussions of the study results would be presented in the future. The overall objective is to provide more precise and accurate windshear and turbulence alerting services in different kinds of weather conditions, by further increasing the hit rate, if possible, and yet reducing the false alarm rate and alert duration in comparison with both pilot reports and aircraft data.

Acknowledgments

The author gratefully acknowledges the support of Cathay Pacific Airways Ltd and Dragonair which provided the QAR data used in this study and the assistance of pilots for filing windshear reports to HKO for the purpose of enhancing flight safety.

References

Chan, P.W., 2009: Performance and application of a multi-wavelength, ground-based microwave radiometer in intense convective weather. *Meteorologische Zeitschrift*, **18**, 253-265.

Chan, P.W., and H. Haverdings, 2009: Quick access recorder (QAR) data analysis software for windshear and turbulence studies. *1st AIAA Atmospheric and Space Environments Conference*, 22 - 25 June 2009, San Antonio, Texas, USA.

Chan, P.W., and K.M. Kwong, 2008: Performance of LIDAR-based turbulence detection algorithm. *13th Conference on Aviation, Range and Aerospace Meteorology*, New Orleans, Louisiana, USA, 20-24 January 2008.

Shun, C.M., and P.W. Chan, 2008: Applications of an infrared Doppler LIDAR in detection of windshear. *J. Atmos. Ocean. Tech.*, **25,** 637 – 655.

Zhang, P., P.W. Chan, R.J. Doviak, and M. Fang, 2009: Estimate of eddy dissipation rate using spectrum width observed by the Hong Kong TDWR radar. *34th Conference on Radar Meteorology*, Williamsburg, Virginia, USA, 5 – 9 October 2009.

period: 2009-01-01 to 05-31	South Runway				
	07RD			25LD	
	Existing	>3km cut off		Existing	>3km cut off
No. of significant windshear reports	78	78		29	29
No. of hits	53	52		24	24
No. of null windshear reports	109	109		67	67
No. of null reports matched with alerts	26	26		65	17
Alert duration (minutes)	12475	8502		25242	16525
Hit rate (%)	68	67		83	83
Alert duration per hit (minutes)	235.38	163.50		1051.75	688.54
False alarm rate (%)	33	33		73	41

Table 1 Performance of LIWAS for departure runway corridors between January and May 2009.

period: 2009-01-01 to 05-31	South runway		North runway	
	07RA	25LA	07LA	25RA
No. of significant windshear reports	69	15	295	71
No. of hits	57	12	227	25
No. of null windshear reports	15	0	159	51
No. of null reports matched with alerts	11	0	118	35
Alert duration (minutes)	17014	8899	15084	2206
Hit rate (%)	83	80	77	35
Alert duration per hit (minutes)	298.49	741.58	66.45	88.24
False alarm rate (%)	16	0	34	58

Table 2 Performance of LIWAS for arrival runway corridors between January and May 2009.

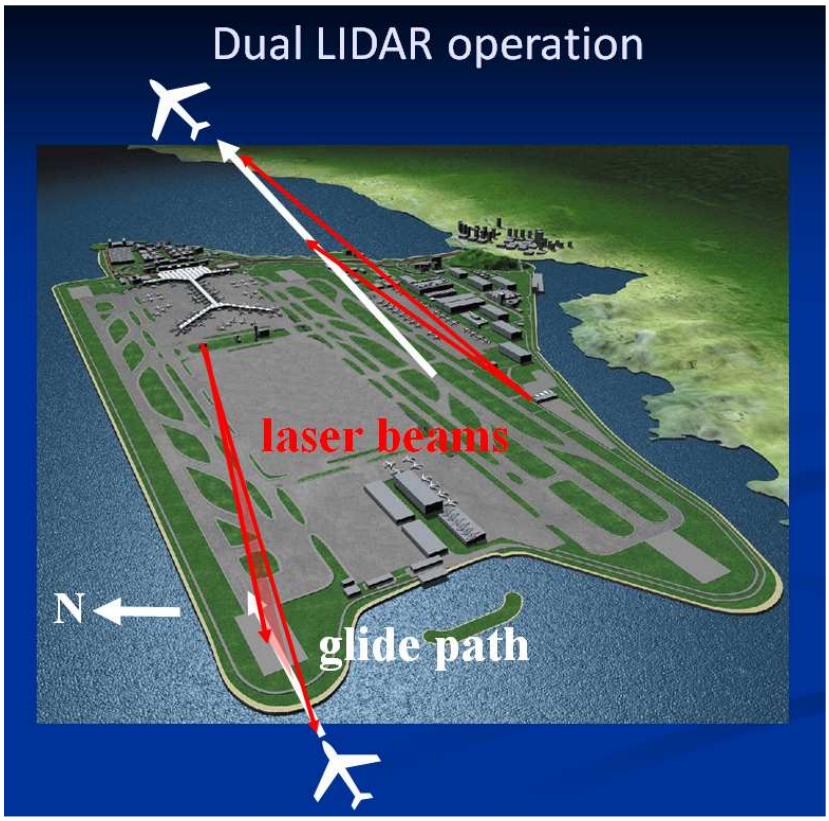

Figure 1 A schematic diagram of dual LIWAS at the Hong Kong International Airport.

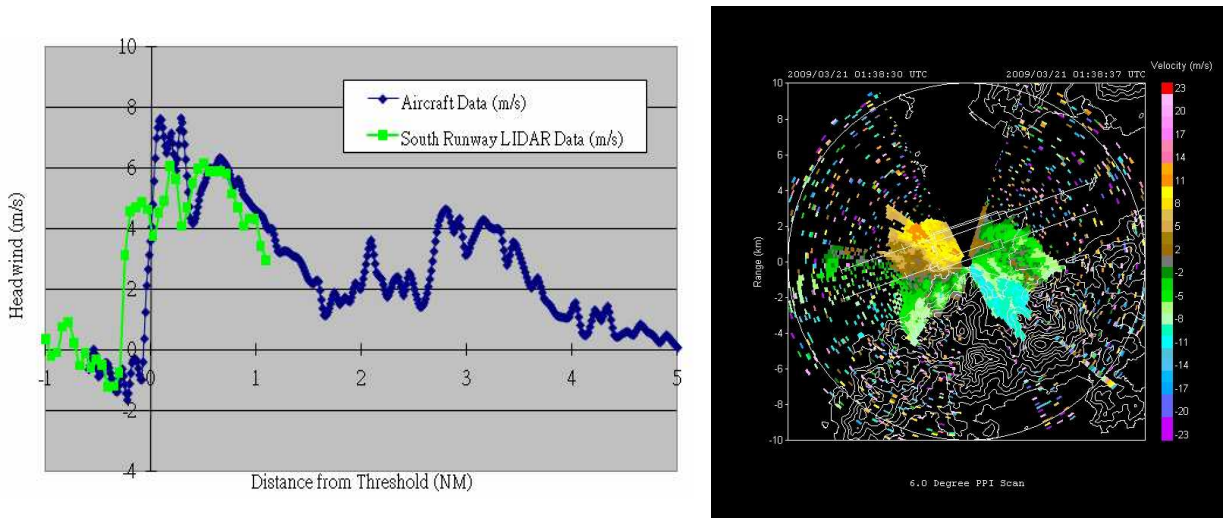

(a) Headwind change measured by the LIDAR is slightly less than that encountered by the aircraft, e.g. 0139 UTC, 21 March 2009 (B744, windshear +15 knots, 400-500 feet)

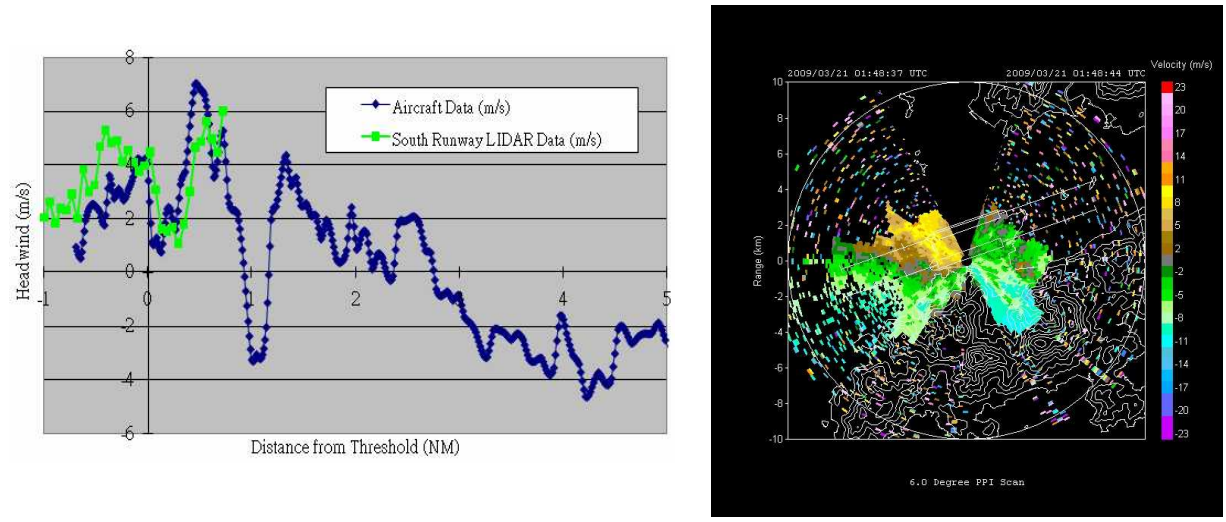

(b) Measurement range of the LIDAR is limited due to low clouds, e.g. 0149 UTC, 21 March 2009 (A333, windshear -20 to -30 knots, 1500 feet)

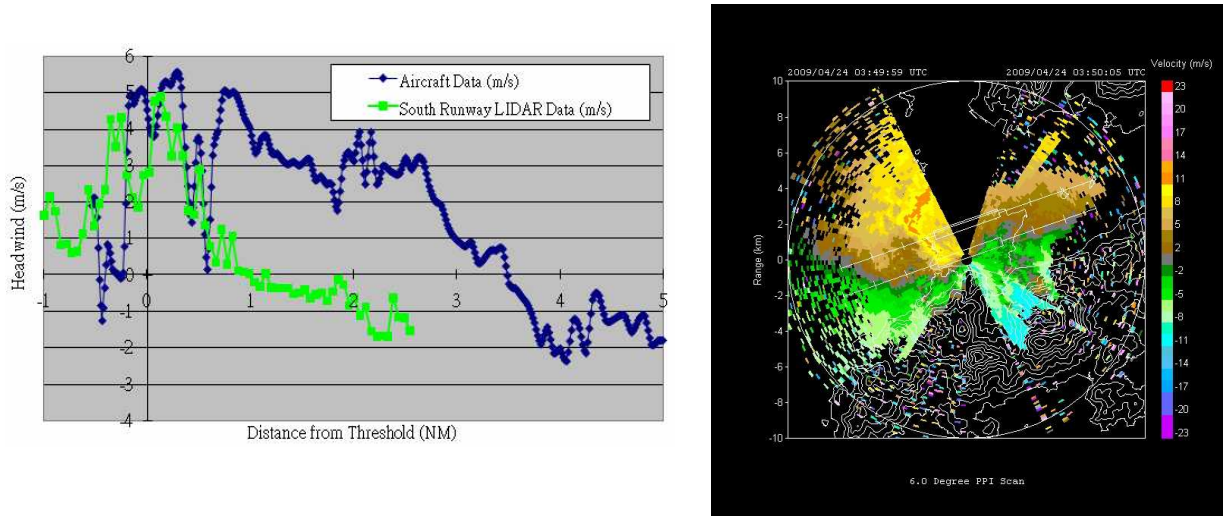

(c) Both aircraft and LIDAR data do not show significant windshear (wind change reaching 15 knots or more), e.g. 0350 UTC, 24 April 2009 (B744, windshear -20 knots, 500 feet)

Figure 2 Some examples of missed cases of LIWAS over 07RD. The headwind profiles (from the aircraft data and the LIDAR data) are shown on the left hand side. The corresponding 6-degree PPI scans of the south runway LIDAR are shown on the right hand side.

(a) The microwave radiometer at the Hong Kong International Airport

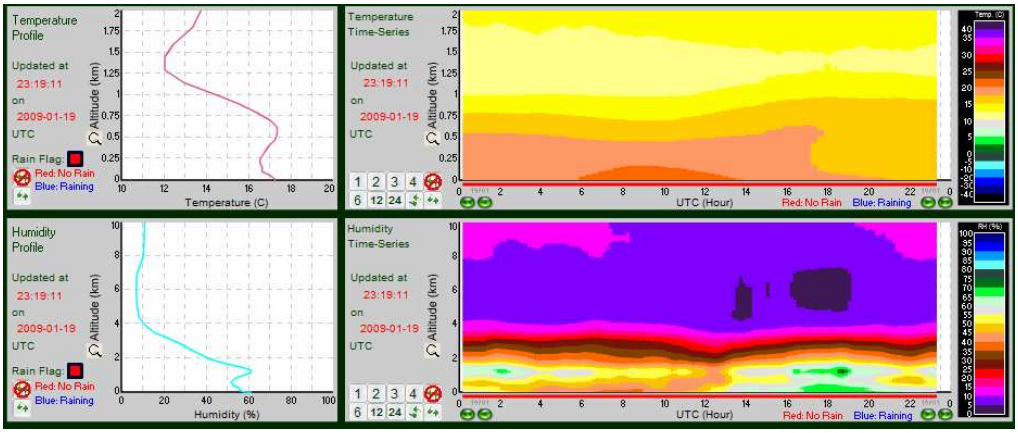

(b) Temperature and humidity profiles (left) and height-time contour plots (right) of the radiometer during the windshear event on 20 January 2009

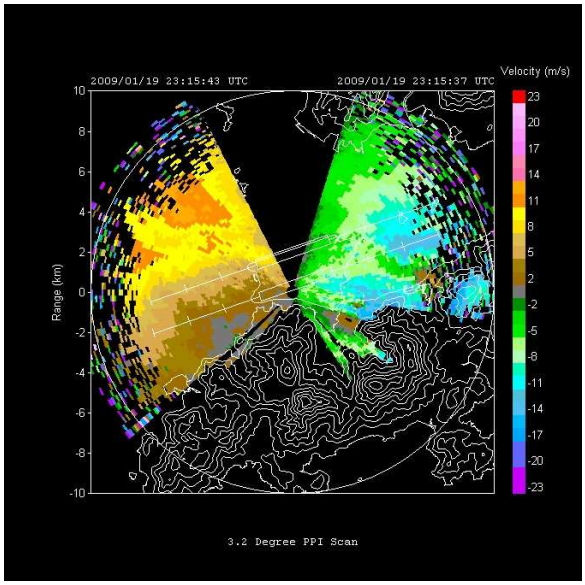

(c) 3.2-degree PPI scan of the south runway LIDAR during the windshear event on 20 January 2009

Figure 3 The microwave radiometer at the airport is shown in (a). The radiometer and LIDAR observations during the windshear event on 20 Jaunary 2009 are shown in (b) and (c) respectively.

(a) The short-range LIDAR on the rooftop of an exhibition centre at the Hong Kong International Airport

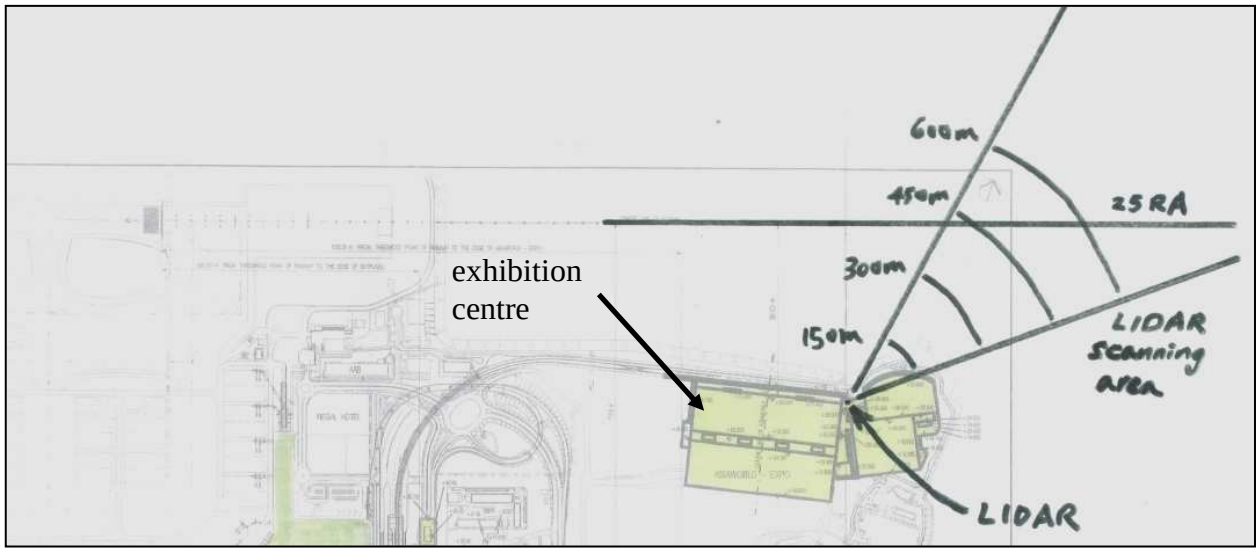

(b) The locations of the short-range LIDAR and 25RA glide path

Figure 4 The short-range LIDAR installed on the rooftop of a building at the Hong Kong International Airport during the low level wind study in the summer 2009: (a) appearance of the LIDAR, and (b) locations of the LIDAR and the corresponding glide path of the aircraft.

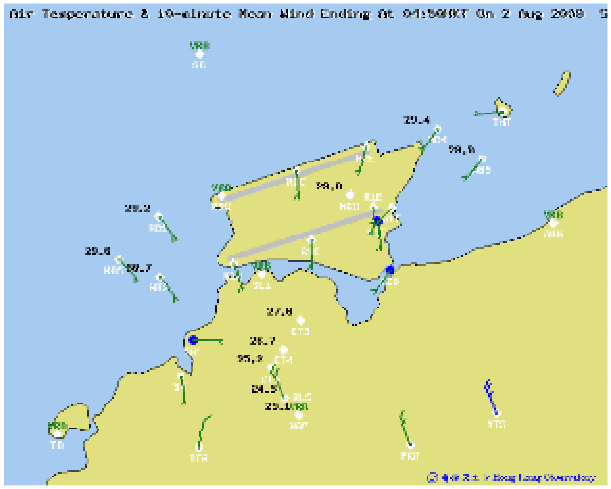

(a) Surface wind distribution at 04:50 HKT, 2 August 2009

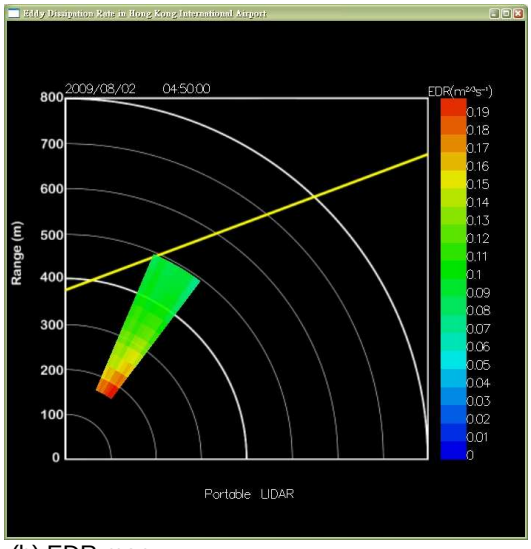

(b) EDR map
(based on LIDAR data between 04:45 – 04:50 HKT)

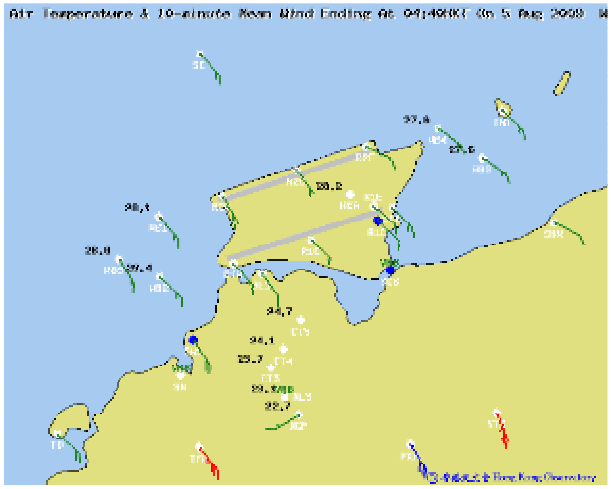

(c) Surface wind distribution at 04:40 HKT, 5 August 2009

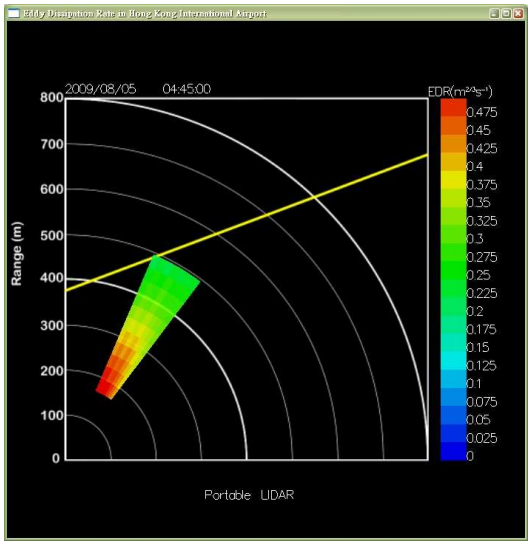

(d) EDR map
(based on LIDAR data between 04:40 – 04:45 HKT)

Figure 5 Two examples of EDR map calculated from the data of the short-range LIDAR. The 25RA glide path is shown as a yellow line in (b) and (d). The wind directions at these times could be seen in (a) and (c).

Figure 6 The locations of the TDWR (red dot) and Hong Kong International Airport (HKIA). The blue beams illustrate the radar beams over the runways corridor 07LA of the airport with 1° azimuth interval. Three yellow lines indicate the approach paths and their names are marked.

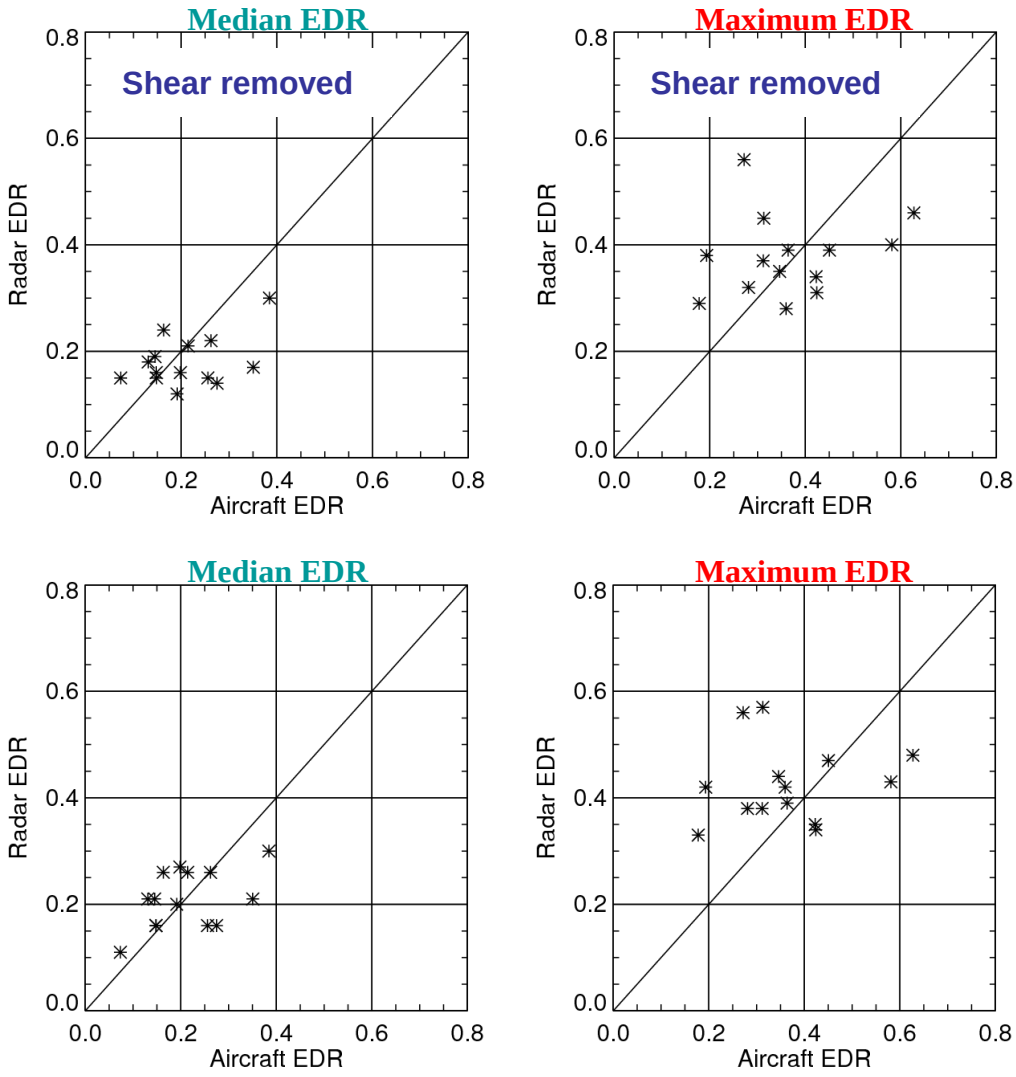

Figure 7 Scatter plots of median and maximum EDR estimated by aircraft and radar along the 5 nm of flight paths for the selected 14 cases.

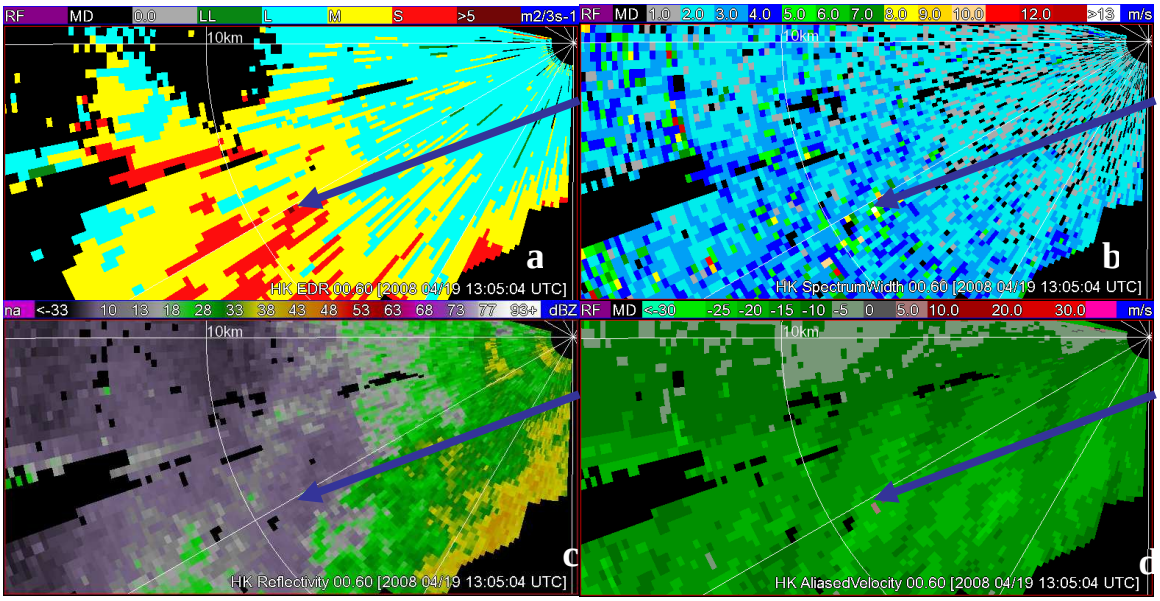

Figure 8 The TDWR data: (a) EDR, (b) spectrum width, (c) reflectivity factor, and (d) Doppler velocity at elevation angle of 0.6° at 13:05 UTC on 19 April 2008. Range ring is at 10 km. Blue arrow line indicates the 5 nm approach path to runway 25RA with length of 5 nm. End of the runway is at the tip of arrow.

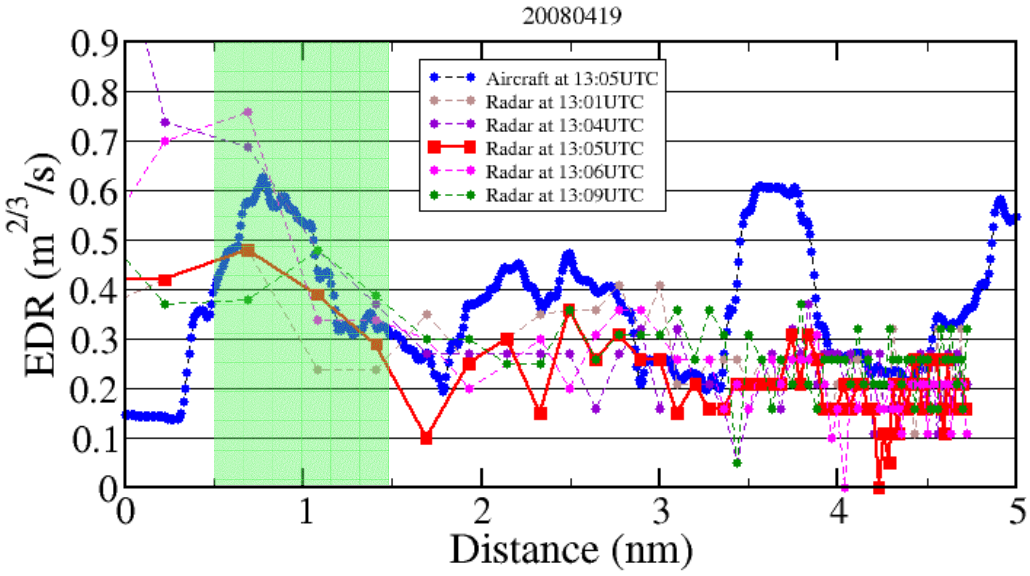

Figure 9 EDR along the flight path estimated by the aircraft B777 (blue dots) over 25RA runway corridor at 13:05 UTC and by the TDWR radar at the time indicated in the legend on 19 April 2008. X axis is the distance between aircraft and the end of runway. The distance interval shaded by the green colour indicates where the aircraft passes through the altitude interval observed with the 0.6° elevated beam.

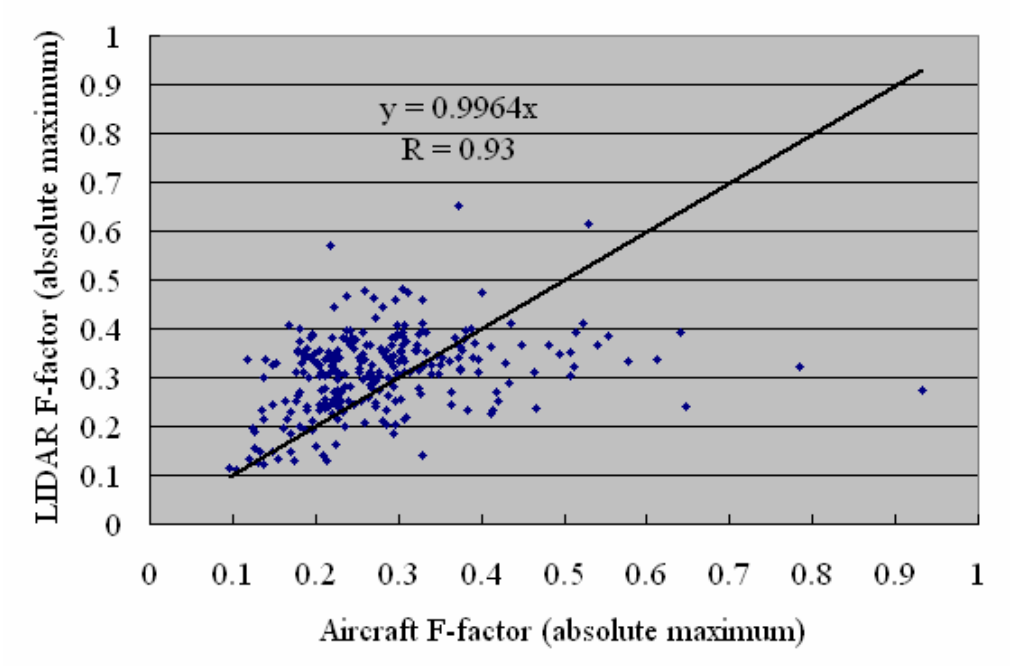

(a)

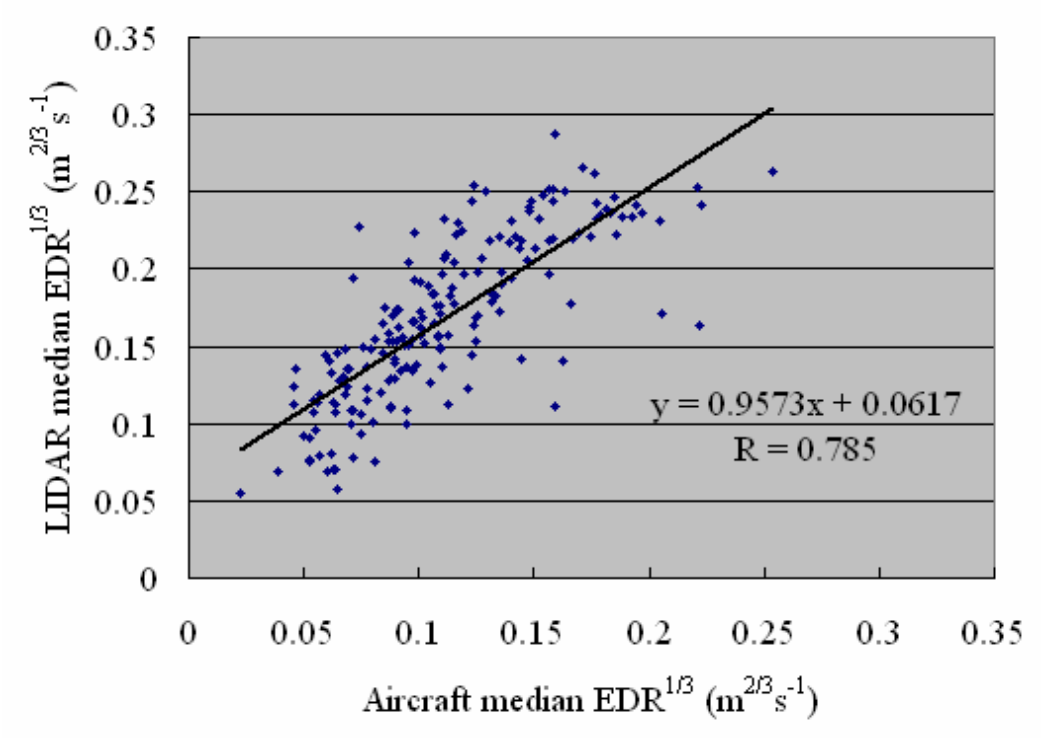

(b)

Figure 10 (a) is the comparison of F-factor values (absolute maximum over the last 4 nautical miles on approach) from the aircraft and from the LIDAR. (b) is the comparison of $EDR^{1/3}$ values (median over the last 4 nautical miles on approach) from the aircraft and from the LIDAR.

(a)

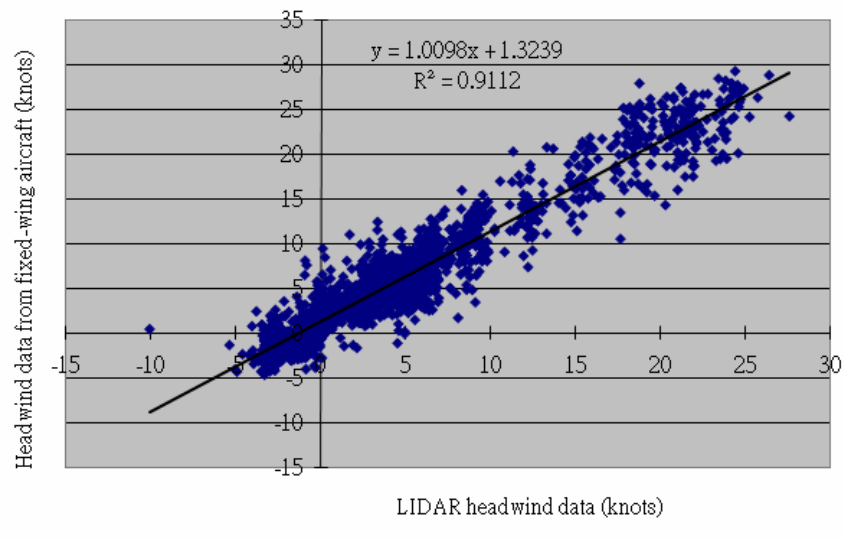

(b)

Figure 11 (a) The AIMMS-20 system installed on the fixed-wing aircraft in Hong Kong (zoom-in view of the air data probe and a GPS antenna could be found in the inset), and (b) comparison between the headwind data measured by the LIDAR and the fixed-wing aircraft between 20 August and 24 September 2009.